VOL. 12, NO. 23, DECEMBER 2017 ISSN 1819-6608
ARPN Journal of Engineering and Applied Sciences

www.arpnjournals.com

BOUNDARY DOMINATED FLOW IN LOW PERMEABILITY RESERVOIR WITH THRESHOLD PRESSURE GRADIENT

Jing Lu[1], Fu Dai[1], Md Motiur Rahman[1] and Freddy Humberto Escobar[2]
[1]Department of Petroleum Engineering, Khalifa University of Science and Technology, Abu Dhabi, United Arab Emirates
[2]Universidad Surcolombiana/CENIGAA, Avenida Pastrana, Neiva, Huila, Colombia
E-Mail: fescobar@usco.edu.co

ABSTRACT

Due to the extremely complicated pore structures and strong fluid-rock interaction, fluid flow in low permeability reservoir does not obey Darcy's law. It is non-Darcy flow associated with threshold pressure gradient. Threshold pressure gradient (*TPG)* is the level of pressure gradient that has to be attained to enable fluid to overcome the viscous forces and start flowing. So, applying traditional well-testing theory in low permeability reservoir will lead to incorrect understanding of reservoir behavior; then, a new mathematical model for describing fluid flow in low permeability reservoir should be established. In non-Darcy flow in low permeability reservoirs, the fluid flow boundary is controlled by threshold pressure gradient and extended outward continuously as production goes on, while reservoir outside this boundary remains to original conditions. Once the moving boundary reaches physical reservoir boundary, it is called boundary dominated flow. This paper presents new mathematical models for boundary dominated flow under two different conditions: constant pressure boundary and closed boundary. Analytical solutions are obtained by using Greens' function with a numerical approximation. It is concluded that, during transient flow, the pressure derivative is not a horizontal line but a concave curve which goes upwards. The bigger threshold pressure gradient brings bigger flow resistance, so the slower pressure wave propagates, and the later boundary dominated flow starts. During boundary dominated flow, the pressure derivative is independent of threshold pressure gradient. A numerical simulation is carried out to validate the analytical solution and approves the validity of the analytical solution. The solution proposed in this paper provides a suggestive tool for well-testing in low permeability reservoir with threshold pressure gradient.

Keywords: well pressure behavior, constant-flow boundary, closed boundary, pseudosteady-state period.

1. INTRODUCTION

Well testing offers an important tool for understanding hydrocarbons properties and characteristic of underground reservoir where oil and gas are trapped. In many years, Darcy's law has been taken as the fundamental equation that governs the fluid flow in porous media, and provides the starting point of well testing theory. However, many experiments show that fluid flow does not obey Darcy's law in low permeability reservoirs, Prada and Civan, 1999; Zeng *et al*., (2011), indicating non-Darcy flow associated with threshold pressure gradient(*TPG*). The reasons for non-Darcy flow in ultra-low permeability reservoirs (K=(0.1-1.0)×10^{-3}μm^2) can be summarized as: strong fluid-rock interaction due to extremely narrow pore throat and large rock surface, obvious boundary-layer flow which varies with the different pressure gradient.

The *TPG* is defined as the pressure gradient that has to be attained for fluid to start flowing. When the pressure gradient is smaller than *TPG*, flow velocity increases in a non-linear relationship, when pressure gradient exceeds *TPG*, flow velocity increases quickly and obeys linear relationship. The existence of *TPG* separates reservoir into two parts, pressure disturbance area, and undisturbed area. The boundary between the two areas is called moving boundary. Before the moving boundary reaches physical reservoir boundary; it is transient flow, after that, boundary dominated flow is dealt with.

Substantial research has been done on transient flow in low permeability reservoir with *TPG* by predecessors. Pascal (1980) firstly studied the transient flow in a one-dimensional model with *TPG*, and derived the approximate analytical solution. Basnyev (1986) proposed a semi-analytical solution for transient radial flow with *TPG* based on material balance equations. Lu (2011) developed a model to describe transient flow in a radial geometry reservoir and obtained a solution with Green's function, which high order of accuracy.

However, few studies are performed for boundary dominated flow in low permeability reservoir with *TPG*. In some cases, well testing is carried out in latter filed life for reservoir management, during which time there is boundary dominated flow. So developing a mathematical model for boundary dominated flow and obtaining analytical solution are quite important. Among the well testing researches can be mentioned: the work of Escobar *et al.* (2014) on horizontal wells draining either homogeneous or naturally fractured formations. Another work by Escobar *et al.* (2015) on hydraulically-fractured vertical wells and Zhao *et al*. (2915) who studied the effect of wellbore storage on the *TPG* for vertical wells.

The purposes of this paper are (1) to present a new mathematical model for boundary dominated flow in radial shape geometry and develop analytical solutions, both constant pressure boundary and closed boundary condition are considered; (2) to illustrate the effects of reservoir parameters on flow behavior, such as *TPG* and permeability, and validate the analytical solution with the numerical simulation.

2. MODEL DEVELOPMENT

Consider the flow configuration as depicted in Figure-1. Flow in this geometry is described in a cylindrical coordinate system with its origin located just right at the center of the well.

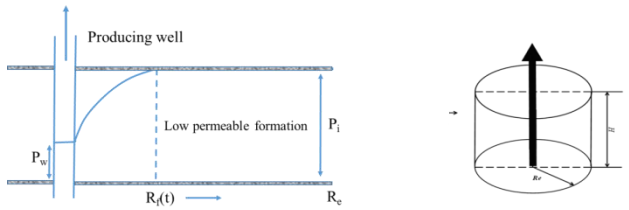

Figure-1. Schematic of a fully penetrating vertical well in the center of an isotropic reservoir.

The following assumptions are made in order to simplify the problem:

a) The well fully penetrates the reservoir with a radius r_w. The reservoir is homogeneous and isotropic with constant permeability, K and porosity, ϕ. The top and the bottom boundary are impermeable.

b) There contains a slightly compressible single-phase fluid with viscosity, μ. The reservoir temperature is constant. The reservoir rock is slightly compressible.

c) Gravity force is negligible. Skin factor is zero. Wellbore storage effect is ignored because of the small wellbore radius.

d) The fluid flow in the formation is governed by non-Darcy flow associated with *TPG*. The reservoir fluid is produced through the fully penetrated well at a constant surface flow rate Q_o. The wellbore radius is so small compared with reservoir radius that it's treated as a line source well.

The fluid flow in low permeability reservoir with *TPG* is described by following non-Darcy flow equation; Prada and Civan (1999), Hao *et al*., (2008),

$$\frac{\partial P}{\partial r} = \left(\frac{\mu}{K}\right)\nu + \omega \qquad (\nu > 0) \tag{1}$$

$$\frac{\partial P}{\partial r} \le \omega \qquad (\nu = 0) \tag{2}$$

where ν is defined as threshold pressure gradient, effective permeability, fluid viscosity, and flow velocity through porous media respectively.

The pressure diffusivity equation in low permeable porous media is,

$$\frac{\partial^2 P}{\partial r^2} + \frac{1}{r}\frac{\partial P}{\partial r} - \frac{\omega}{r} = \frac{\phi \mu C_t}{K}\frac{\partial P}{\partial t} \tag{3}$$

Where ϕ, C_t are respectively the porosity and total compressibility of low permeability formation.

The focus of this paper is to establish a mathematical model for boundary dominated flow and obtain the analytical solution, the pressure when boundary dominated flow starts is the exact reservoir pressure when moving boundary just reaches the physical outer boundary, it can be obtained from the pressure transient solution by Lu (2011).

$$P(r,t)\big|_{t=t_e} = P_e \tag{4}$$

Where P_e is the pressure when moving boundary reaches the physical outer boundary, t_e is the time that moving boundary reaches the physical boundary.

For closed boundary situation, there is no fluid supply into the reservoir, so the pressure at outer boundary keeps declining at a constant rate.

$$\left.\frac{\partial P}{\partial r}\right|_t = C \tag{5}$$

Where C is a constant.

For constant pressure boundary situation, the pressure at the outer boundary keeps the same with original reservoir pressure.

$$P(r,t)\big|_{r=r_e} = P_i \tag{6}$$

The inner boundary conditions for both closed boundary and constant pressure boundary problem are the same,

$$\left(\frac{K}{\mu}\right)\left.\frac{\partial P}{\partial r}\right|_{r=R_w} - \omega) = \frac{BQ_o}{2\pi H R_w} \tag{7}$$

The well is taken as a uniform line sink and it is a fully penetrating well, a point sink (0, 0,0) is located at the origin of the polar coordinates, its intensity is q, q has the same dimensional unit as the total well flow rate Q_o, and Q_o keeps constant during production.

$$Q_o = qH_D = q\left(\frac{H}{R_w}\right) \tag{8}$$

Then equation can be expressed as:

$$\frac{\partial^2 P}{\partial r^2} + \frac{1}{r}\frac{\partial P}{\partial r} - \frac{\omega}{r} = \frac{\phi \mu C_t}{K}\frac{\partial P}{\partial t} + \frac{\mu q B \delta(r)}{2\pi K H r} \tag{9}$$

Where $\delta(r)$ is Dirac delta function.

2.1. Dimensionless transform

For simplifying the process of equation derivation, dimensionless parameters are introduced into equations,

$$r_D = \frac{r}{R_w} \tag{10}$$

$$t_D = \frac{Kt}{\phi\mu C_t R_w^2} \tag{11}$$

$$P_D = \frac{KR_w(P_i - P)}{\mu qB} = \frac{KR_w(P_i - P)H_D}{\mu Q_o B} = \frac{KH(P_i - P)}{\mu Q_o B} \tag{12}$$

$$\omega_D = \frac{K\omega R_w^2}{\mu qB} = \frac{K\omega H_D R_w^2}{\mu Q_w B} = \frac{K\omega H R_w}{\mu Q_w B} \tag{13}$$

Consequently, equation(9) can be expressed in the following dimensionless form,

$$\frac{\partial^2 P_D}{\partial r_D{}^2} + \frac{1}{r_D}\frac{\partial P_D}{\partial r_D} + \frac{\omega_D}{r_D} = \frac{1}{r_D}\frac{\partial}{\partial r_D}(r_D\frac{\partial P_D}{\partial r_D}) + \frac{\omega_D}{r_D} = \frac{\partial P_D}{\partial t_D} - \frac{\delta(r_D)}{2\pi H_D r_D} \tag{14}$$

Where the following formula is used,

$$\delta(r) = \delta(r_D R_w) = \frac{\delta(r_D)}{R_w} \tag{15}$$

The boundary condition for a closed boundary and constant pressure boundary can be expressed as below respectively.

$$P|_{t=0} = 0 \tag{16}$$

$$P|_{r=R_f} = 0 \tag{17}$$

$$\frac{\partial P}{\partial r}|_{r=R_f} = -\omega \tag{18}$$

Where R_f is moving boundary front.

For convenience, every variable, domain, initial and boundary conditions would be taken as dimensionless, but we drop the subscript D for simplicity.

2.2. Analytical solution using Green's function

Define the following parameter and drop subscript D for simplicity,

$$\psi = P + \omega r \tag{19}$$

Consequently,

$$\frac{1}{r}\frac{\partial}{\partial r}(r\frac{\partial(\omega r)}{\partial r}) = \frac{1}{r}\frac{\partial(\omega r)}{\partial r} = \frac{\omega}{r}\frac{\partial r}{\partial r} = \frac{\omega}{r} \tag{20}$$

$$\frac{\partial\psi}{\partial t} = \frac{\partial P}{\partial t} + \frac{\partial(\omega r)}{\partial t} = \frac{\partial P}{\partial t} + 0 = \frac{\partial P}{\partial t} \tag{21}$$

Thus, we obtain following equations about Ψ,

$$\frac{\partial\psi}{\partial t} - \frac{1}{r}\frac{\partial}{\partial r}(r\frac{\partial\psi}{\partial r}) = \frac{\delta(r)}{2\pi Hr} \tag{22}$$

$$\psi|_{t=0} = \omega r \tag{23}$$

$$\frac{\partial\psi}{\partial r}|_{r=R_f} = \frac{\partial P}{\partial r}|_{r=R_f} + \frac{\partial(\omega r)}{\partial r} = -\omega + \omega = 0 \tag{24}$$

G is the Green's function of the above problem, there hold,

$$\begin{cases} \frac{\partial G}{\partial t} - \frac{1}{r}\frac{\partial}{\partial r}(r\frac{\partial G}{\partial r}) = \frac{\delta(t-\tau)\delta(r-\rho)}{2\pi r} \\ G|_{t=0} = 0 \\ \frac{\partial G}{\partial r}|_{r=R_f} = 0 \end{cases} \tag{25}$$

Using the method of undetermined coefficients, it is assumed that moving boundary location at time t is R_f, so the solution can be derived using Green's function. Thus the solution to Equation (25) is:

$$\begin{aligned} \psi(R_f, t, r) &= I_1 + I_2 \\ &= \frac{1}{\pi HR_f^2}\left\{t + \sum_{n=1}^{\infty} R_f^2\left[\frac{1-\exp(-\lambda_n^2 t/R_f^2)}{\lambda_n^2}\right]\left[\frac{J_0(\lambda_n r/R_f}{[J_0(\lambda_n)]^2}\right]\right\} \\ &+ (2\omega R_f)\left\{\frac{1}{3} + \sum_{n=1}^{\infty}\exp(-\lambda_n^2 t/R_f^2)\frac{\sigma_n J_0(\lambda_n r/R_f}{[J_0(\lambda_n)]^2}\right\} \end{aligned} \tag{26}$$

Lu(2011) gave the detailed pressure solution for transient flow, so the detail is not given here. The solution is shown below,

$$t_e = \frac{\pi H\omega R_e^3}{3} \tag{27}$$

In which t_e is the time that moving boundary reaches physical boundary and boundary dominated flow starts.

The pressure transient at t_e is as follows, and engineering accuracy could be attained by considering one hundred terms of the summations (n=1 to n=100).

$$\psi_e(r)=\psi(R_e,t_e,r)$$
$$=(\frac{1}{\pi HR_e^2})\left\{t_e+\sum_{n=1}^{100}R_e^2\left[\left(\frac{1-\exp(-\lambda_n^2t_e/R_e^2}{\lambda_n^2}\right)\frac{J_0(\lambda_nR_w/R_e)}{[J_0(\lambda_n)]^2}\right]\right\}$$
$$+(2\omega R_f)\left\{\frac{1}{3}+\sum_{n=1}^{100}\left[\frac{\sigma_nJ_0(\lambda_nr/R_e)\exp(-\lambda_n^2t_e/R_e^2)}{[J_0(\lambda_n)]^2}\right]\right\} \quad (28)$$

Equation(28) is the initial pressure condition of for boundary dominated flow problem.

$$\frac{\partial\psi}{\partial t}-\frac{1}{r}\frac{\partial}{\partial r}(r\frac{\partial\psi}{\partial r})=\frac{\delta(r)}{2\pi Hr} \quad (29)$$

$$\psi|_{t=0}=\psi_e(r) \quad (30)$$

2.3. Closed outer boundary

If the reservoir is with closed outer boundary, it is known that $\partial P/\partial r=0$ at $r=R_e$.

$$\frac{\partial\psi}{\partial r}|_{r=R_e}=\frac{\partial P}{\partial r}|_{r=R_e}+\frac{\partial(\omega r)}{\partial r}=0+\omega=\omega \quad (31)$$

It is Newman boundary condition for this case. The Green's function for Newman boundary can be found in page 438 of Cole *et al*. (2010).

$$\psi(R_e,t;r)=\int_0^t\int_0^{2\pi}\int_0^{\mathrm{Re}}G(t,r,\tau,p)\left[\frac{\delta(\rho)}{2\pi\rho H}\right]\rho d\rho d\tau d\phi$$
$$+\int_0^{2\pi}\int_0^{R_e}G(t,r,0,\rho)[\psi_e(\rho)]\rho d\rho d\phi+\int_0^t 2\pi R_e\omega G(t,R_e,\tau,r)d\tau \quad (32)$$
$$=\int_0^tG(t,r,\tau,0)d\tau/H+(2\pi)\int_0^{R_e}G(t,r,0,\rho)[\psi_e(\rho)]\rho d\rho$$
$$+(2\pi R_e\omega)\int_0^tG(t,R_e,\tau,r)d\tau$$
$$=I_1+I_2+I_3$$

Where;

$$I_1=\int_0^tG(t,r,\tau,0)d\tau/H$$
$$=\int_0^t(\frac{1}{\pi HR_e^2})\left\{1+\sum_{n=1}^{100}\exp\left[-\lambda_n^2(t-\tau)/R_e^2\right]\left[\frac{J_0(\lambda_nr/R_e)}{[J_0(\lambda_n)]^2}\right]\right\}d\tau \quad (33)$$
$$=\left(\frac{1}{\pi HR_e^2}\right)\left\{t+\sum_{n=1}^{100}R_e^2\left[\frac{1-\exp(-\lambda_n^2t/R_e^2)}{\lambda_n^2}\right]\left[\frac{J_0(\lambda_nr/R_e)}{[J_0(\lambda_n)]^2}\right]\right\}$$

Where λ_n (n=1,2,3, …) are roots of the following equation:

$$J_1(\lambda_n)=0,\quad (n=1,2,3,...) \quad (34)$$

$$I_2=(2\pi)\int_0^{R_e}G(t,r,0,\rho)[\psi_e(\rho)]\rho d\rho$$
$$=(2\pi)\int_0^{R_e}\left\{\left(\frac{1}{\pi R_e^2}\right)\left\{1+\sum_{n=1}^{100}\exp\left[-\lambda_n^2t/R_e^2\right]\frac{J_0(\lambda_nr/R_e)J_0(\lambda_n\rho/R_e)}{[J_0(\lambda_n)]^2}\right\}\right\}$$
$$\times\left\{\begin{array}{l}\left(\frac{1}{\pi HR_e^2}\right)\left\{t_e+\sum_{n=1}^{100}R_e^2\left[\frac{1-\exp(-\lambda_n^2t_e/R_e^2)}{\lambda_n^2}\right]\left[\frac{J_0(\lambda_nr/R_e)}{[J_0(\lambda_n)]^2}\right]\right\}\\+(2\omega R_e)\left\{\frac{1}{3}+\sum_{n=1}^{100}\exp(-\lambda_n^2t_e/R_e^2)\frac{\sigma_nJ_0(\lambda_nr/R_e)}{[J_0(\lambda_n)]^2}\right\}\end{array}\right\}\rho d\rho \quad (35)$$

Note that in Equation(35),

$$\sigma_n=\int_0^1J_0(\lambda_nx)x^2dx \quad (36)$$

$$I_3=(2\pi R_e\omega)\int_0^tG(t,R_e,\tau,r)d\tau$$
$$=(2\pi R_e\omega)\int_0^t\left\{\left(\frac{1}{\pi R_e^2}\right)\left\{1+\sum_{n=1}^{100}\exp\left[-\lambda_n^2(t-\tau)/R_e^2\right]\frac{J_0(\lambda_nr/R_e)J_0(\lambda_nR_e/R_e)}{[J_0(\lambda_n)]^2}\right\}\right\}d\tau \quad (37)$$
$$=(2\pi R_e\omega)\left(\frac{1}{\pi R_e^2}\right)\left\{t+\sum_{n=1}^{100}\frac{J_0(\lambda_nr/R_e)J_0(\lambda_n)}{[J_0(\lambda_n)]^2}\left[\frac{R_e^2}{\lambda_n^2}(1-\exp(-\lambda_n^2t/R_e^2))\right]\right\}$$
$$=\left(\frac{2\omega}{R_e}\right)\left\{t+\sum_{n=1}^{100}\frac{J_0(\lambda_nr/R_e)}{[J_0(\lambda_n)]}\left[\frac{R_e^2}{\lambda_n^2}(1-\exp(-\lambda_n^2t/R_e^2))\right]\right\}$$

2.4. Constant pressure outer boundary

For constant outer boundary condition, the pressure at $r=R_e$ always equals to reservoir initial pressure P_i, according to dimensionless pressure definition, we have:

$$P_e=0 \quad (38)$$

This boundary condition is called Dirichlet boundary. Consequently,

$$\psi_e=P_e+\omega R_e=0+\omega R_e=\omega R_e \quad (39)$$

We consider the following problem:

$$\frac{\partial\psi}{\partial t}-\frac{1}{r}\frac{\partial}{\partial r}(r\frac{\partial\psi}{\partial r})=\frac{\delta(r)}{2\pi Hr} \quad (40)$$

$$\psi|_{t=0}=\psi_e(r) \quad (41)$$

$$\psi_e=P_e+\omega R_e=0+\omega R_e=\omega R_e \quad (42)$$

If G is the Green's function for the problem above, there hold:

$$\begin{cases}\frac{\partial G}{\partial t}-\frac{1}{r}\frac{\partial}{\partial r}(r\frac{\partial G}{\partial r})=\frac{\delta(t-\tau)\delta(r-\rho)}{2\pi r}\\G|_{t=0}=0\\\frac{\partial G}{\partial r}|_{r=R_e}=0\end{cases} \quad (43)$$

For the Green's function, there holds,

$$G(t,r;\tau,r') = \frac{1}{\pi R_e^2}\left\{\sum_{n=1}^{\infty}\exp(-\beta_n^2(t-\tau)/R_e^2)\frac{J_0(\beta_n r/R_e)J_0(\beta_n r'/R_e)}{[J_1(\beta_n)]^2}\right\} \quad (44)$$

Where β_n(n=1,2,3, ...) are the roots of Bessel function of zero order,

$$J_0(\beta_n) = 0, (n = 1, 2, 3, \ldots) \quad (45)$$

Green's function for Dirichlet boundary can be found in in page 437 of Cole *et al*. (2010).

$$\begin{aligned}\psi(R_e,t;r) &= \int_0^t\int_0^{2\pi}\int_0^{R_e} G(t,r,\tau,p)\left[\frac{\delta(\rho)}{2\pi\rho H}\right]\rho d\rho d\tau d\phi \\ &+\int_0^{2\pi}\int_0^{R_e} G(t,r,0,\rho)[\psi_e(\rho)]\rho d\rho d\phi + \int_0^t 2\pi R_e\omega G(t,R_e,\tau,r)d\tau \\ &= \int_0^t G(t,r,\tau,0)d\tau/H + (2\pi)\int_0^{R_e} G(t,r,0,\rho)[\psi_e(\rho)]\rho d\rho \\ &+(2\pi R_e\omega)\int_0^t G(t,R_e,\tau,r)d\tau \\ &= I_1 + I_2 + I_3\end{aligned} \quad (46)$$

$$\begin{aligned}I_1 &= \int_0^t G(t,r,\tau,0)d\tau/H \\ &= \int_0^t\left(\frac{1}{\pi H R_e^2}\right)\left\{\sum_{n=1}^{100}\exp\left[-\beta_n^2(t-\tau)/R_e^2\right]\left[\frac{J_0(\beta_n r/R_e)}{[J_1(\beta_n)]^2}\right]\right\}d\tau \\ &= \left(\frac{1}{\pi H R_e^2}\right)\left\{\sum_{n=1}^{100}R_e^2\left[\frac{1-\exp(-\beta_n^2 t/R_e^2)}{\beta_n^2}\right]\left[\frac{J_0(\beta_n r/R_e)}{[J_1(\beta_n)]^2}\right]\right\}\end{aligned} \quad (47)$$

$$\begin{aligned}&I_2 \\ &= (2\pi)\int_0^{R_e} G(t,r,0,\rho)[\psi_e(\rho)]\rho d\rho \\ &= (2\pi)\int_0^{R_e}\left\{\left(\frac{1}{\pi R_e^2}\right)\left\{\sum_{n=1}^{100}\exp\left[-\beta_n^2 t/R_e^2\right]\frac{J_0(\beta_n r/R_e)J_0(\beta_n\rho/R_e)}{[J_1(\beta_n)]^2}\right\}\right\} \\ &\times\left\{\begin{array}{l}\left(\frac{1}{\pi H R_e^2}\right)\left\{t_e + \sum_{n=1}^{100}R_e^2\left[\frac{1-\exp(-\lambda_n^2 t_e/R_e^2)}{\lambda_n^2}\right]\left[\frac{J_0(\lambda_n r/R_e)}{[J_0(\lambda_n)]^2}\right]\right\} \\ +(2\omega R_e)\left\{\frac{1}{3}+\sum_{n=1}^{100}\exp(-\lambda_n^2 t_e/R_e^2)\frac{\sigma_n J_0(\lambda_n\rho/R_e)}{[J_0(\lambda_n)]^2}\right\}\end{array}\right\}\rho d\rho\end{aligned} \quad (48)$$

Where;

$$\sigma_n = \int_0^1 J_0(\lambda_n x)x^2 dx \quad (49)$$

$$\begin{aligned}I_3 &= (2\pi R_e\omega)\int_0^t G(t,R_e,\tau,r)d\tau \\ &= (2\pi R_e\omega)\int_0^t\left\{\left(\frac{1}{\pi R_e^2}\right)\left\{\sum_{n=1}^{100}\exp\left[-\beta_n^2(t-\tau)/R_e^2\right]\frac{J_0(\beta_n r/R_e)J_0(\beta_n R_e/R_e)}{[J_1(\beta_n)]^2}\right\}\right\}d\tau \\ &= (2\pi R_e\omega)\left(\frac{1}{\pi R_e^2}\right)\left\{\sum_{n=1}^{100}\frac{J_0(\beta_n r/R_e)J_0(\lambda_n)}{[J_1(\beta_n)]^2}\left[\frac{R_e^2}{\beta_n^2}(1-\exp(-\beta_n^2 t/R_e^2))\right]\right\} \\ &= \left(\frac{2\omega}{R_e}\right)\left\{\sum_{n=1}^{100}\frac{J_0(\beta_n r/R_e)J_0(\lambda_n)}{[J_1(\beta_n)]^2}\left[\frac{R_e^2}{\beta_n^2}(1-\exp(-\beta_n^2 t/R_e^2))\right]\right\}\end{aligned} \quad (50)$$

2.5. Transform from dimensionless solutions into dimensional solutions

Incorporating the dimensionless parameters into the dimensionless analytical solutions for boundary dominated flow, and obtaining the dimensional solutions of pressure distribution in the reservoir. The results are shown below in SI unit.

2.5.1. Closed outer boundary

$$P(R_e,t,r) = P_i - \frac{\mu Q_o B}{KH}(I_1 + I_2 + I_3) + \omega r \quad (51)$$

Where:

$$I_1 = \left(\frac{R_w}{\pi H R_e^2}\right)\left\{\frac{Kt}{\phi\mu C_t} + \sum_{n=1}^{100}R_e^2\left[\frac{1-\exp(-\lambda_n^2\frac{Kt}{\phi\mu C_t R_e^2})}{\lambda_n^2}\right]\left[\frac{J_0(\lambda_n r/R_e)}{[J_0(\lambda_n)]^2}\right]\right\} \quad (52)$$

$$\begin{aligned}&I_2 \\ &= (2\pi)\int_0^{R_e}\left\{\left(\frac{1}{\pi R_e^2}\right)\left\{1+\sum_{n=1}^{100}\exp\left[-\lambda_n^2\frac{Kt}{\phi\mu C_t R_e^2}\right]\frac{J_0(\lambda_n r/R_e)J_0(\lambda_n\rho/R_e)}{[J_0(\lambda_n)]^2}\right\}\right\} \\ &\times\left\{\begin{array}{l}\left(\frac{R_w^3}{\pi H R_e^2}\right)\left\{\frac{Kt_e}{\phi\mu C_t R_w^2}+\sum_{n=1}^{100}\frac{R_e^2}{R_w^2}\left[\frac{1-\exp(-\lambda_n^2\frac{Kt_e}{\phi\mu C_t R_e^2})}{\lambda_n^2}\right]\left[\frac{J_0(\lambda_n r/R_e)}{[J_0(\lambda_n)]^2}\right]\right\} \\ +\left(2\frac{K\omega H R_e}{\mu Q_o B}\right)\left\{\frac{1}{3}+\sum_{n=1}^{100}\exp(-\lambda_n^2\frac{Kt_e}{\phi\mu C_t R_e^2})\frac{\sigma_n J_0(\lambda_n r/R_e)}{[J_0(\lambda_n)]^2}\right\}\end{array}\right\}\rho d\rho\end{aligned} \quad (53)$$

$$I_3 = \left(\frac{2K\omega H R_w^2}{\mu Q_o B R_e}\right)\left\{\frac{Kt}{\phi\mu C_t R_w^2} + \sum_{n=1}^{100}\frac{\frac{J_0(\lambda_n r/R_e)}{[J_0(\lambda_n)]}}{\left[\frac{R_e^2}{\lambda_n^2 R_w^2}(1-\exp(-\lambda_n^2\frac{Kt}{\phi\mu C_t R_e^2}))\right]}\right\} \quad (54)$$

2.5.2. Constant pressure outer boundary

$$P(R_e,t,r) = P_i - \frac{\mu Q_o B}{KH}(I_1 + I_2 + I_3) + \omega r \quad (55)$$

$$I_1 = \left(\frac{R_w}{\pi H}\right)\left\{\sum_{n=1}^{100}\left[\frac{1-\exp(-\beta_n^2\frac{Kt}{\phi\mu C_t R_e^2})}{\beta_n^2}\right]\left[\frac{J_0(\beta_n r/R_e)}{[J_1(\beta_n)]^2}\right]\right\} \quad (56)$$

$$\begin{aligned}&I_2 \\ &= (2\pi)\int_0^{R_e}\left\{\left(\frac{1}{\pi R_e^2}\right)\left\{\sum_{n=1}^{100}\exp\left[-\beta_n^2\frac{Kt}{\phi\mu C_t R_e^2}\right]\frac{J_0(\beta_n r/R_e)J_0(\beta_n\rho/R_e)}{[J_1(\beta_n)]^2}\right\}\right\} \\ &\times\left\{\begin{array}{l}\left(\frac{R_w^3}{\pi H R_e^2}\right)\left\{\frac{Kt_e}{\phi\mu C_t R_w^2}+\sum_{n=1}^{100}\frac{R_e^2}{R_w^2}\left[\frac{1-\exp(-\lambda_n^2\frac{Kt_e}{\phi\mu C_t R_e^2})}{\lambda_n^2}\right]\left[\frac{J_0(\lambda_n r/R_e)}{[J_0(\lambda_n)]^2}\right]\right\} \\ +\left(2\frac{K\omega H R_e}{\mu Q_o B}\right)\left\{\frac{1}{3}+\sum_{n=1}^{100}\exp(-\lambda_n^2\frac{Kt_e}{\phi\mu C_t R_e^2})\frac{\sigma_n J_0(\lambda_n\rho/R_e)}{[J_0(\lambda_n)]^2}\right\}\end{array}\right\}\rho d\rho\end{aligned} \quad (57)$$

$$I_3 = \left(\frac{2K\omega HR_w^2}{\mu Q_o BR_e}\right)\left\{\sum_{n=1}^{100}\frac{J_0(\beta_n r/R_e)J_0(\lambda_n)}{[J_1(\beta_n)]^2}\left[\frac{R_e^2}{\beta_n^2 R_w^2}(1-\exp(-\beta_n^2\frac{Kt}{\phi\mu C_t R_e^2}))\right]\right\} \quad (58)$$

3. PRESSURE BEHAVIOR ANALYSIS

By using the new mathematical models for boundary dominated flow, parameter sensitivity on pressure and production behavior are studied. These models for non-Darcy flow with threshold pressure gradient are also compared with the traditional Darcy's flow model, in order to reveal the pressure behavior difference during production.

3.1. Closed boundary

Figure-2 shows the effect of threshold pressure gradient on pressure P_{wD} and pressure derivative $P_{wD}'t_D$, and it's compared with that of Darcy's flow.

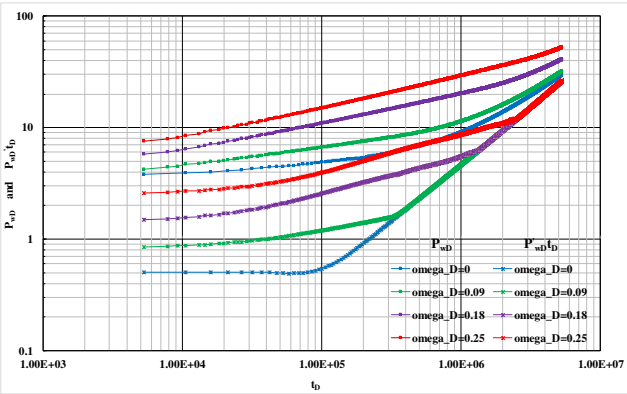

Figure-2. Log-log plot of dimensionless bottomhole pressure and pressure derivative vs. dimensionless time t_D in boundary dominated flow period with closed boundary.

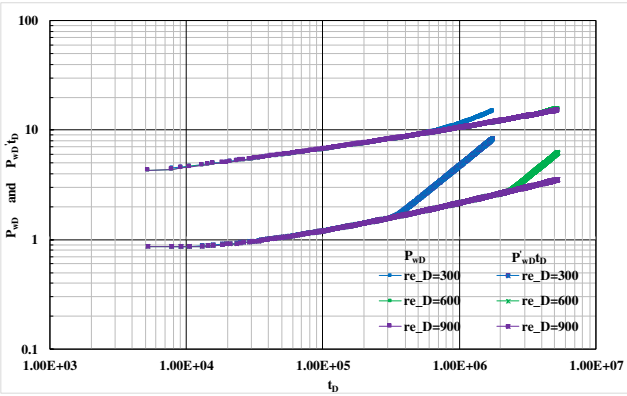

Figure-3. Log-log plot of dimensionless bottomhole pressure and pressure derivative vs. dimensionless time t_D in boundary dominated flow period with closed boundary (ω_D=0.09).

The curves for all the four cases can be divided into two regimes, early-middle time regime, and late time regime. For ω_D=0, which is Darcy's flow, P_{wD} is smallest among all the four cases, it indicates that the flow resistance for Darcy's flow is smallest, the pressure derivative $P_{wD}'t_D$ is a horizontal line and equals to 0.5 in early-middle time regime, in late time regime, as the moving boundary reaches physical boundary, the pressure derivative $P_{wD}'t_D$ start to derivate from horizontal line, pressure drop speed increases. For all cases $\omega_D \neq 0$, As $\omega_D$increase from 0.09 to 0.25, the P_{wD} increase, the pressure derivative $P_{wD}'t_D$ derivate from the horizontal line, the bigger ω_D is, the more $P_{wD}'t_D$deviates from the horizontal line. It is seen that in pressure derivative curve, as $\omega_D$increase, the latter the turning point of $P_{wD}'t_D$ appears, so the latter boundary dominated flow appears.

For Figure-3, the curves for all the four cases can be divided into two regimes, early-middle time regime and late time regime. It is seen that the bigger r_{eD} is, the later $P_{wD}'t_D$ starts to increase, indicating that the later steady-state flow appears.

3.2. Constant pressure boundary

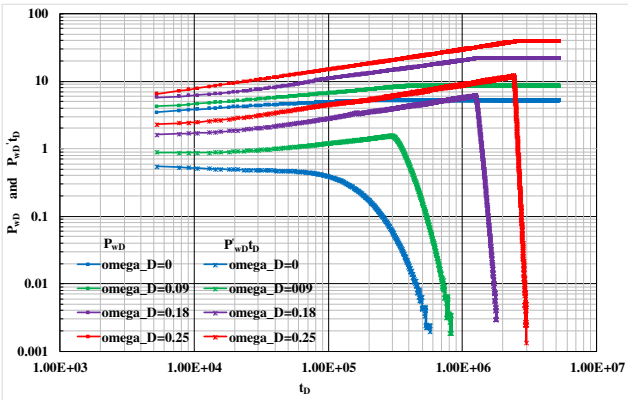

Figure-4. Log-log plot of dimensionless bottomhole pressure and pressure derivative vs. dimensionless time $t_D$in boundary dominated flow period with constant pressure boundary.

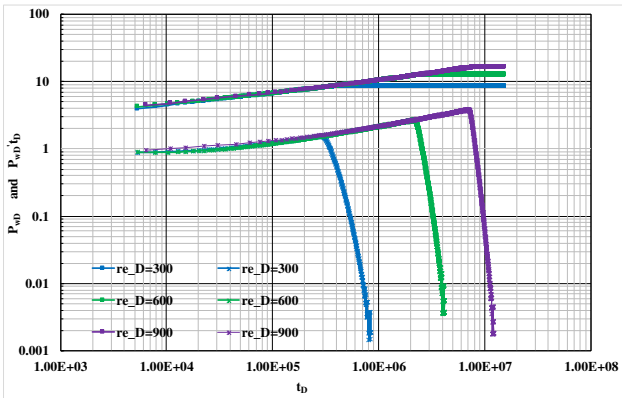

Figure-5. Log-log plot of dimensionless bottomhole pressure and pressure derivative vs. dimensionless time t_D in boundary dominated flow period with constant pressure boundary (ω_D=0.09).

It is seen that the bigger r_{eD} is, the later $P_{wD}^{'} t_D$ starts to decrease, indicating that the later steady-state flow appears. See Figures4 and 5.

4. COMPARISON WITH SIMULATION RESULT

Validation of the new mathematical models is achieved by comparing it with numerical simulation result. A radial geometry flow model with 100*1*1 grids is constructed to simulate the pressure distribution in a reservoir associated with threshold pressure gradient, and the grid dimensions in radial, theta, **z** directions are 3 ft, 360°, 20ft respectively, as shown in Figure-6. The production well is located in the grid (1,1,1). The model formation properties and fluid properties are listed in Table-1.

The keyword THPRES sets the threshold pressure for flow between adjacent equilibration regions, fluid in grids which belong to different equilibration regions will not start to flow unless the pressure difference between these grids is bigger than the threshold pressure value set by THPRES keyword. A case of ω=20 psi/ft are studied.

4.1. Closed boundary

Plotting the pressure versus time on Cartesian plot, and comparing it with the analytical solution. The result is shown in Figure-7. It is seen that analytical solution curve matches with simulation run curve well, error range is smaller than 10 %.

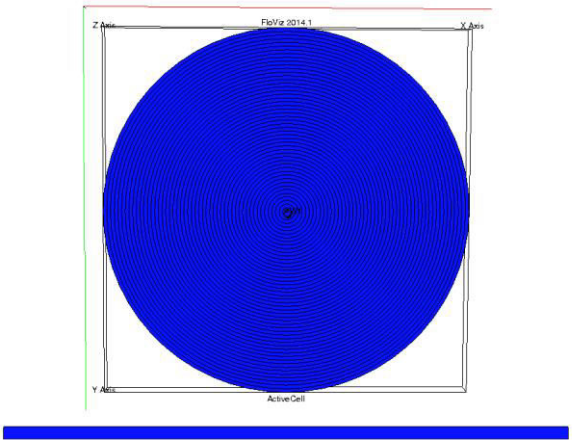

Figure-6. Schematic of mesh generation in a circular reservoir.

Table-1. Formation properties of the radial model.

Parameters	Value
Reservoir radius, R_e	150 ft
Reservoir Thickness, H	20 ft
Porosity, ϕ	0.1
radial permeability, k_r	0.5 mD
azimuthal permeability, k_θ	0.5 mD
Z-permeability, k_z	0.5 mD
Oil compressibility, C_o	2E-5 1/psi
Oil FVF, B_o	1.25
Oil viscosity, μ_o	0.5 cp
Formation compressibility	2E-5 1/psi
Threshold pressure gradient ω	0, 5, 15, 25 psi/ft

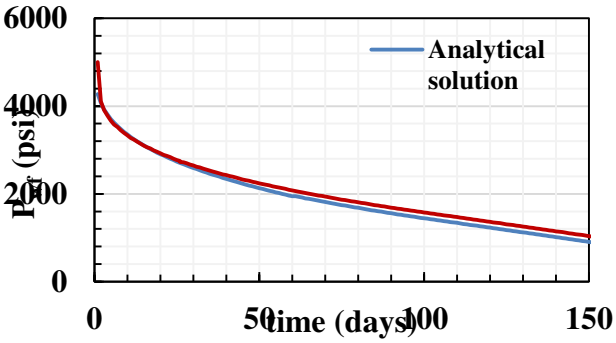

Figure-7. Cartesian plot of bottomhole pressure vstime for Analytical model and Eclipse simulation run (ω=20 psi/ft).

4.2. Constant pressure boundary

Fetkovich aquifer model is employed to simulation the constant pressure boundary. AQUFET keyword is used in Eclipse data file to specify the Fetkovich aquifer. The pressure for Fetkovich aquifer is equal to initial reservoir pressure.

Pressure versus time on Cartesian plot is shown in Figure-8. It is seen that analytical solution curve matches with simulation run curve well. Bottomhole pressure does not decrease anymore when it reaches constant pressure boundary.

VOL. 12, NO. 23, DECEMBER 2017 ISSN 1819-6608
ARPN Journal of Engineering and Applied Sciences

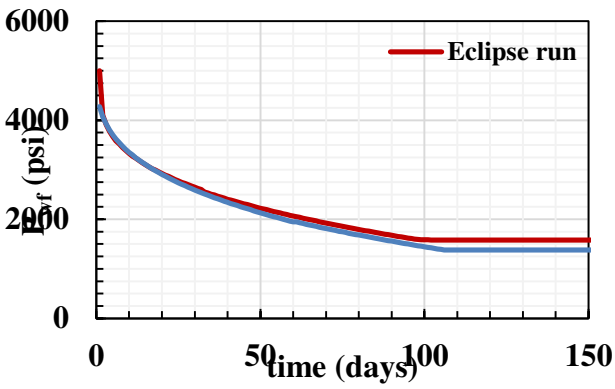

Figure-8. Cartesian plot of bottomhole pressure vs time for Analytical model and Eclipse simulation run(ω=20 psi/ft).

CONCLUSIONS

For the model of transient flow, the bottomhole pressure behavior, moving boundary front position, and pressure distribution in the reservoir are investigated. The conclusions are as shown below:

a) The threshold pressure gradient ω is defined as the level of pressure gradient that has to be attained to enable the fluid to overcome the viscous forces and start to flow when the pressure draw-down acts on that fluid medium. It widely exists in low permeability reservoir.
b) The bigger threshold pressure gradient ω is, the bigger pressure drop it need to make the fluid start flowing, which will lead to bigger pressure drop will be in the reservoir and bottomhole.
c) The existence of threshold pressure gradient intensifies the uneven distribution of pressure along radial distance, more pressure drop happens around the wellbore.
d) The moving boundary front position R_f is linear relationship with $t^{1/3}$, and it is a function of production rate, threshold pressure gradient, porosity, formation thickness, but not a function of permeability.
e) Bottomhole pressure P_{wf} is a linear relationship with $t^{1/3}$, the bigger threshold pressure gradient ω is, the bigger bottomhole pressure drop in the well is.
f) The bigger threshold pressure gradient ω is, the later the moving boundary front reaches physical boundary, the later the transient flow finish and boundary dominated flow to start.
g) For the boundary dominated flow, there are two cases: closed boundary condition and constant pressure boundary condition. The bottomhole pressure behavior, moving boundary front position, and pressure distribution in the reservoir are investigated. The conclusions are as shown below.

For closed boundary condition:

a) It becomes a pseudo-steady state if production time is long enough. At each point of the reservoir, the pressure drop is the same per unit time.

b) The bigger threshold pressure gradient ω is, the bigger pressure drop speed is when in pseudo-steady state flow.

For constant pressure boundary condition:

c) It becomes a steady state if production time is long enough. The pressure distribution in the reservoir will not change if the well producing at a constant rate.

Nomenclature

A	flow area of wellbore
K	effective permeability
P	pressure
r	radial distance
G	Green's function
C_t	total compressibility
h	thickness
t	time
B	formation volume factor
H	pay zone thickness
R_w	wellbore radius
R_f	moving boundary front
R_e	reservoir outer boundary
Q_o	oil flow rate
Greek symbols	
$\delta(r)$	Dirac delta function
μ	Fluid viscosity
λn	nth root of $J_1(x)=0$
βn	nth root of $J_0(x)=0$
ω	Threshold pressure gradient
ϕ	Porosity
Subscripts	
D	Dimensionless
f	moving boundary front
e	reservoir outer boundary
o	oil
i	initial
w	well

Appendix A: Dimensional factors table			
Factor	**Dimension**	**SI units**	**Field units**
Distance	L	m	ft
Area	L^2	m^2	acre
Temperature	T	Kelvin	Rankine
Pressure	$mL^{-1}t^{-2}$	Pa	psi
Permeability	L^2	m^2	mD
Viscosity	$mL^{-1}t^{-1}$	Pa.s	cp
Flow rate	L^3t^{-1}	m^3s^{-1}	MMSCF/day
Pseudo pressure	mL^1t^{-3}	Pa/s	$(MMpsi)^2/cp$

ACKNOWLEDGEMENTS

The authors would like to thank the senior management of Abu Dhabi National Oil Company and The Petroleum Institute in Abu Dhabi for their continuous support and for permission to publish this work.

REFERENCES

Civan F. 2011. Porous Media Transport Phenomena. John Wiley & Sons Press.

Chen M., Rossen W. and Yortsos Y.C. 2005. The Flow and Displacement in Porous Media of Fluids with Yield Stress. Chemical Engineering Science. 60(15):4183-4202.

Datta-Gupta A., Xie J., Gupta N., King M. J.& Lee W. J. 2011, July 1. Radius of Investigation and its Generalization to Unconventional Reservoirs. Society of Petroleum Engineers. doi:10.2118/0711-0052-JPT.

Escobar F.H., Zhao Y.L. and Zhang L.H. 2014. Interpretation of Pressure Tests in Horizontal Wells in Homogeneous and Heterogeneous Reservoirs with Threshold Pressure Gradient. Journal of Engineering and Applied Sciences. 9(11): 2220-2228.

Escobar F.H., Zhao Y.L., Pournik M., Liu Q.G. and Olaya-Marin G. 2015. Interpretation of Pressure Tests in Uniform-Flux Fractured Vertical Wells with Threshold Pressure Gradient in Low Permeability Reservoirs. Journal of Engineering and Applied Sciences. 10(20): 9364-9372.

Finjord J. & Aadnoy B. S. 1989, September 1. Effects of the Quadratic Gradient Term in Steady-State and Semisteady-State Solutions for Reservoir Pressure. SPE Formation Evaluation. 4(3):413-417. Society of Petroleum Engineers. doi:10.2118/15969-PA.

Hagoort J. 2004, June 1. Non-Darcy Flow Near Hydraulically Fractured Wells. Societyof Petroleum Engineers. doi:10.2118/80419-PA.

Lee J., Rollins J.B. and Spivey J. P. 2003. Pressure Transient Testing, SPE Textbook Series, ISBN:978-089520-317-5, Society of Petroleum Engineers.

Kuchuk F. J. 2009, January 1. Radius of Investigation for Reserve Estimation from Pressure Transient Well Tests. Society of Petroleum Engineers. doi:10.2118/120515-MS.

Cole K.V., Beck J.V., Haji-Sheikh A. and Litkouhi B. 2010. Heat Conduction Using Green's Functions, 2nd Edition, CRC Press, 2010. Cole, K.V., Beck, J.V., Haji-Sheikh, A. and Litkouhi, B.

Liu W.C, Yao J. and Wang Y. 2012. Exact Analytical Solutions of Moving Boundary Problems of One-Dimensional Flow in Semi-Infinite Long Porous Media with Threshold Pressure Gradient. International Journal of Heat and Mass Transfer. 55: 6017-6022.

Lu J. and Ghedan S. 2011. Pressure Behavior of Vertical Wells in Low-Permeability Reservoirs with Threshold Pressure Gradient. Special Topics & Reviews in Porous Media. 2(3):157-169.

Lu J. 2012.Pressure Behavior of Uniform-Flux Hydraulically Fractured Wells in Low-Permeability Reservoirs with Threshold Pressure Gradient, Special Topics & Reviews in Porous Media. 3(4): 307-320.

Lu J. 2012, January 1. Pressure Behavior of a Hydraulic Fractured Well in Tight Gas Formation with Threshold Pressure Gradient. Society of Petroleum Engineers. doi:10.2118/152158-MS.

Marshall S. 2009. Nonlinear Pressure Diffusion in Flow of Compressible Liquids through Porous Media.Transport in Porous media. 77(3):431-446.

Odeh A. S. and Babu D. K. 1988, November 1. Comparison of Solutions of the Nonlinear and Linearized Diffusion Equations. SPE Reservoir Engineering. 3(4):1202-1206. Society of Petroleum Engineers. doi:10.2118/17270-PA.

Prada A., Civan F. 1999. Modification of Darcy's law for the Threshold Pressure Gradient. Journal of Petroleum Science and Engineering. 22(4): 237-240.

Pascal H. 1981. Non-Steady flow through Porous Media in the Presence of a Threshold Pressure Gradient. Acta Mechanica. 39(3-4):207-224.

Sochi T. 2010. Modeling the Flow of Yield-Stress Fluids in Porous Media. Transport in porous media. 85(2):489-503.

Wu Y.S. 1990. Theoretical Studies of Non-Newtonian and Newtonian Fluid Flow through Porous Media. California: University of California.

Wu Y.-S., Pruess K. and Witherspoon P. A. 1992, August 1. Flow and Displacement of Bingham Non-Newtonian Fluids in Porous Media. SPE reservoir Engineering 1993, 7(3): 369-376. Society of Petroleum Engineers. doi:10.2118/20051-PA.

Wang Y. and Dusseault M.B. 1991. The Effect of Quadratic Gradient Terms on the Borehole Solution in Poro-Elastic Media. Water Resources Research. 27(12): 3215-3223.

Xu J., Jiang R., Xie L., Wang R., Shan L. and Li L. 2012, January 1. Non-Darcy Flow Numerical Simulation for Low-permeability Reservoirs. Society of Petroleum Engineers. doi:10.2118/154890-MS.

Zhao Y.L., Escobar F.H. Jamili A., Olaya-Marin G. and Ghisays-Ruiz A. 2015. Effect of Wellbore Storage on the Vertical Well Pressure Behavior with Threshold Pressure Gradient in Low Permeability Reservoirs. Journal of Engineering and Applied Sciences. 10(22): 10659-10664.

Zeng B., Cheng L. and Li C. 2011. Low-Velocity Non-Linear Flow in Ultra-Low Permeability Reservoir. Journal of Petroleum Science and Engineering. 80(1):1-6.